Iodide Complexes of Decaborane(14) and 2,4-Diiododecaborane(14). The X-ray Crystal Structure of $[P(C_6H_5)_3CH_3][2,4\text{-}I_2B_{10}H_{12}I]$

Joseph R. Wermer,[†] Orin Hollander,[†] John C. Huffman,[‡] Jeanette A. Krause Bauer,[§] Danan Dou,[†] Leh-Yeh Hsu,[†] Daniel L. Leussing,*[,†] and Sheldon G. Shore*[,†]

Department of Chemistry, The Ohio State University, Columbus, Ohio 43210, and Molecular Structure Center, Indiana University, Bloomington, Indiana 47405

Received November 17, 1994[⊗]

A yellow, solid, ion-dipole charge transfer complex, $[M][B_{10}H_{14}I]$, is formed upon mixing the solids [M]I (M = $[N(n\text{-}(C_4H_9)_4]^+$, $[P(C_6H_5)_3CH_3]^+$, $[(Ph_3P)_2N]^+$) and $B_{10}H_{14}$. The $[B_{10}H_{14}I]^-$ ion is stabilized in the solid state by the presence of bulky cations; $B_{10}H_{14}$ cannot be separated by sublimation from the solid. A Job continuous variations experiment establishes that the reaction stoichiometry, a 1:1 molar ratio of $[N(n\text{-}(C_4H_9)_4]I$ to $B_{10}H_{14}$, also occurs in CH_2Cl_2 solution. While there is no apparent reaction when solid alkali metal iodides are mixed with $B_{10}H_{14}$ in the absence of a solvent, addition of an appropriate solvent to the solid mixture causes formation of the $[B_{10}H_{14}I]^-$ anion. However, removal of the solvent causes the complex to revert to a mixture from which $B_{10}H_{14}$ can be removed by sublimation. When $2,4\text{-}I_2B_{10}H_{12}$ is mixed with iodide salts of the cations $[N(n\text{-}C_4H_9)_4]^+$, $[P(C_6H_5)_3CH_3]^+$, $[(Ph_3P)_2N]^+$, Na^+, and K^+ in the absence of a solvent, there is no apparent reaction. However when a suitable solvent is present, the complex anion $[2,4\text{-}I_2B_{10}H_{12}I]^-$ is formed. A single crystal X-ray structure determination of $[P(C_6H_5)_3CH_3][2,4\text{-}I_2B_{10}H_{12}I]$ shows the unique iodide residing on top of the four hydrogen bridge atoms and the 6,9 boron atoms at the opening of the B_{10} basket. Crystal data for $[P(C_6H_5)_3CH_3][2,4\text{-}I_2B_{10}H_{12}I]$: monoclinic $P2_1/c$, a = 12.868(4) Å, b = 10.562(3) Å, c = 22.007(8) Å, β = 99.40(2)°, Z = 4, V = 2950.7 Å^3, R = 3.4%, R_w = 3.6%.

Introduction

While investigating the properties of decaborane(14), we observed the formation of an intensely yellow colored solid product upon mixing the solids $[(n\text{-}C_4H_9)_4N]I$ and $B_{10}H_{14}$. The product of this reaction was found to be sufficiently stable to preclude physical separation of the starting components. Subsequent studies revealed a complex ion $[B_{10}H_{14}I]^-$ for which we know of no precedent in the literature. We describe here the preparation and characterization of $[B_{10}H_{14}I]^-$ and the related anion $[2,4\text{-}I_2B_{10}H_{12}I]^-$.

Results

$[B_{10}H_{14}I]$. Formation of Complex Ions. Decaborane(14) reacts with iodide salts, [M]I to form yellow complexes that have the general molecular formula $[M][B_{10}H_{14}I]$, eq 1. The

$$MI + B_{10}H_{14} \rightarrow M[B_{10}H_{14}I] \qquad (1)$$

$$M = [N(n\text{-}C_4H_9)_4]^+, [P(C_6H_5)_3CH_3]^+, [(C_6H_5)_3P)_2N]^+$$

stabilities of these complexes are highly dependent upon the choice of cation. With the large cation iodide salts given above, the yellow complexes form upon mixing of the solid reactants; the addition of THF or CH_2Cl_2 results in the formation of deep yellow solutions. These complexes are isolated as solid, air stable materials. Solutions show noticeable decomposition in air after a period of several days. The decaborane(14) molecule is tightly bound in these solids. Once the complex is formed and the solvent is removed, decaborane(14), which is normally volatile at room temperature cannot be sublimed from the complex even at 95 °C under vacuum (10^{-3} Torr). Indeed, one way compositions of complexes were established was to use excess $B_{10}H_{14}$ in the preparative reactions and to then sublime away from the reaction mixture the uncomplexed $B_{10}H_{14}$ and weigh it.

While large complex counterions stabilize $[B_{10}H_{14}I]^-$ in the solid state, apparently this anion is not formed when an alkali metal iodide is mixed with $B_{10}H_{14}$ in the absence of a solvent. However, in solution (THF for NaI, EtOH for KI) $[B_{10}H_{14}I]^-$ is formed, but upon removal of solvent the complex reverts to a mixture from which $B_{10}H_{14}$ is readily sublimed.

Job Titrations. The complex ion $[B_{10}H_{14}I]^-$ absorbs in the visible region at 355 nm in CH_2Cl_2. The position of the maximum is independent of the cation and the sample concentration. Neither $B_{10}H_{14}$ nor any of the iodide salts used as cations show significant absorption in the visible region. The formation of $[(n\text{-}C_4H_9)_4N][B_{10}H_{14}I]$ in CH_2Cl_2 was followed by a Job titration experiment[1] in which the absorbance maximum of the complex was monitored under the conditions $[B_{10}] + [(TBAI)] = 0.002M$, where $[B_{10}]$ = molar concentration of $B_{10}H_{14}$ and [(TBA)I] = molar concentration of $[(n\text{-}C_4H_9)_4N]I$ at temperatures of 250, 268, 281 K. Plots of absorbance *vs* mole fraction of TBAI are given in Figure 1. The well-defined maxima, evident at a mole fraction of 0.5 at all temperatures, are consistent with a combining ratio of 1:1, eq 2.

$$TBA^+I^- + B_{10}H_{14} \overset{\beta_1}{\rightleftharpoons} TBA^+B_{10}H_{14}I^- \qquad (2)$$

The data were subjected to nonlinear curve-fitting to test the the accuracy of this model and to obtain the values of the formation constants and molar absorbancies. In addition to the

[†] The Ohio State University.
[‡] Indiana University.
[§] Present address: Department of Chemistry, University of Cincinnati, Cincinnati, Ohio 45221.
[⊗] Abstract published in *Advance ACS Abstracts*, April 15, 1995.

(1) (a) Denision, R. B. *Trans. Faraday Soc.* **1912**, 8, 20; **1912**, 8, 35. (b) Job, P. *Ann. Chim. Paris* **1928**, 9, 113.

0020-1669/95/1334-3065$09.00/0

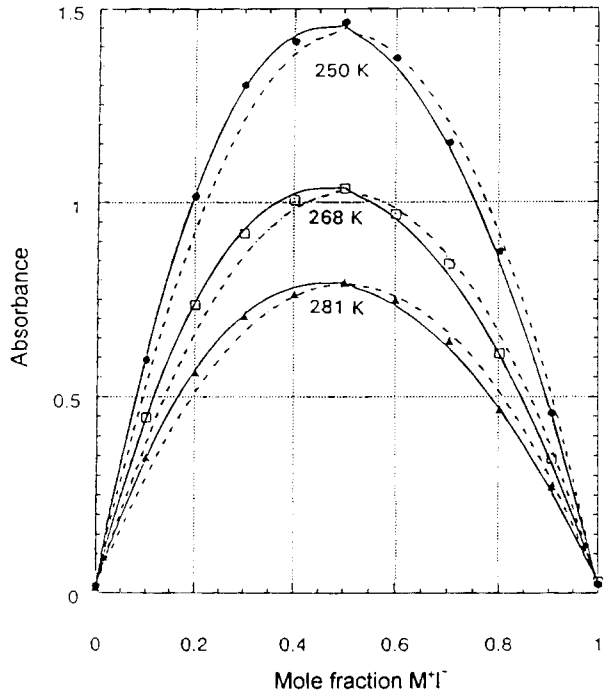

------ = least squares plot of primary equilibrium.
—— = least squares plot of primary and secondary equilibria.

Figure 1. Plots of absorbance *vs* mole fraction of TBAI.

equilibrium constraint defined by eq 2, mass balance was also invoked. Values of $[B_{10}H_{14}]_{tot}$ and $[TAB^+I^-]_{tot}$ are known for each data point, so when a value of β_1 is assumed it is possible to solve for the corresponding equilibrium concentrations of the species defined on the right hand side of eqs 3 and 4. The

$$[B_{10}H_{14}]_{tot} = [B_{10}H_{14}] + [TBA^+B_{10}H_{14}I^-] \quad (3)$$

$$[TBA^+I]_{tot} = [TBA^+I^-] + [TBA^+B_{10}H_{14}I^-] \quad (4)$$

Newton–Raphson method[2] was employed to solve these nonlinear expressions. Calculated values of absorbance are then obtained using eq 5, where a_i is the molar absorptivity and a_{B10}

$$Abs_{cal} = a_{B10}[B_{10}H_{14}] + a_{TBAI}[TBA^+I^-] + a_{adduct}[TBA^+B_{10}H_{14}I^-] \quad (5)$$

and a_{TABI} were obtained from the absorbancies at the initial and terminal points of the curves shown in Figure 1. An assumed value of a_{adduct} then allows a theoretical absorbance–mole fraction curve to be calculated. Using the Marquardt algorithm,[3] it was then possible to find the values of adduct and β_1 that minimized the function $\sum(Abs_{obs} - Abs_{calc})^2$. The β_1's are temperature dependent and were fit to the data points at each temperature, but it was found possible to use a single a_{adduct} for all three temperatures.

The dashed lines shown in the figure represent the curves calculated using the "best" least-squares values a_{adduct} and β_1 obtained in the fitting process. Although the maxima of the calculated curves agree well with the observed data points, a pronounced deviation of the dashed lines from the observed values is evident at all temperatures.

(2) Press, W. N.; Flannery, B. P.; Teukolsky, S. A.; Vetterling, W. T. *Numerical Recipes*, Cambridge University Press: Cambridge, England, 1986; p 269.
(3) Bevington, P. R.; Robinson, D. K. *Data Reduction and Error Analysis for the Physical Sciences*, 2nd ed.; McGraw-Hil: New York, 1992.

Table 1. Equilibrium Constants for Interactions Involving $B_{10}H_{14}$ and TBA^+I^- in CH_2Cl_2 Solvent

temp (K)	log β_1 (eq 2)	log β_2 (eq 6)
250	2.2(2)	2.2(2)
268	2.0(2)	2.3(2)
281	1.9(2)	2.3(2)

[a] The molar absorptivity of $TBA^+B_{10}H_{14}I^-$ is taken as 1.4×10^4 $M^{-1}cm^{-1}$ from a preliminary fitting procedures.

Because of the well-known penchant of electrolytes to form ion-pairs in solvents of low dielectric constant, a secondary equilibrium eq 6 was incorporated into the model and eqs 4

$$2TAB^+I^- \overset{\beta_2}{\rightleftharpoons} \begin{matrix} TAB^+I^- \\ | \quad | \\ I^-TAB^+ \end{matrix} \quad (6)$$

and 5 were modified to take into account this additional adduct, eqs 7 and 8.

$$[TBA^+I^-]_{tot} = [TBA^+I^-] + 2[(TBA^+I^-)_2] + [TBA^+B_{10}H_{14}I^-] \quad (7)$$

$$Abs_{cal} = a_{B10}[B_{10}H_{14}] + a_{TBAI}[TBA^+I^-] + 2a_{TABI}[TBA^+I^-_2] + a_{adduct}[TBA^+B_{10}H_{14}I^-] \quad (8)$$

The Marquardt[3] algorithm yielded $a_{adduct} = 1.4 \times 10^4$ M^{-1} cm^{-1} with the corresponding temperature dependent values of β_1 and β_2 given in Table 1. The calculated absorbance-mole fraction curves are indicated by the solid lines drawn in Figure 1. Excellent agreement between observed and calculated points is seen to have been attained with this model.

The dependence of log β_1 on temperature is only slightly greater than the errors in the determination of the constants, however, reaction 1 appears to be exothermic with a rough heat of about -3 kcal mol^{-1}. This reaction involves the replacement of a strong ion pair, TAB^+I^-, with one that is weaker because it possesses a considerably larger anion, $[B_{10}H_{14}I]^-$. Thus, the heat of reaction I^- with $B_{10}H_{14}$ in CH_2Cl_2 is suggested to be more exothermic than -3 kcal-mol^{-1}.

It is expected that eq 6 would also exhibit a decreasing equilibrium constant with increasing temperature. However, the dielectric constants of solvents show a decrease with increasing temperature and this factor tends to increase electrostatic interactions with increasing temperature, compensating for the tendency for increased dissociation.[4]

Spectra. The ^{11}B NMR spectrum of $[(C_6H_5)_3P)_2N][B_{10}H_{14}I]$ in CD_2Cl_2 consists of four well resolved doublets at 12.3 (2B), 7.8 (2B), -3.1 (4B), and -33.5 (2B) ppm (Figure 2). The connectivity of boron atoms in the B_{10} cage was confirmed from the 2D $^{11}B-^{11}B$ COSY spectrum shown in Figure 3. The general appearance of the ^{11}B spectrum of $[(C_6H_5)_3P)_2N][B_{10}H_{14}I]$ resembles that of $B_{10}H_{14}$ and is consistent with the apparent C_{2v} point symmetry of the B_{10} cage (Figure 3). However, formation of the iodide complex leads to an upfield shift of the B(1,3) and B(5,7,8,10) signals by 4.4 and 3.8 ppm, respectively, and a downfield shift of the B(6,9) and B(2,4) signals by 1.7 and 2.2 ppm, respectively. This trend is also observed for the other $[M][B_{10}H_{14}I]$ complexes represented in Table 2.

The ^1H NMR spectrum of $[(C_6H_5)_3P)_2N][B_{10}H_{14}I]$ in CD_2Cl_2 (Table 2), assigned by means of selective heteronuclear

(4) Gurney, R. W. *Ionic Processes in Solution*; McGraw-Hill, New York, 1953.

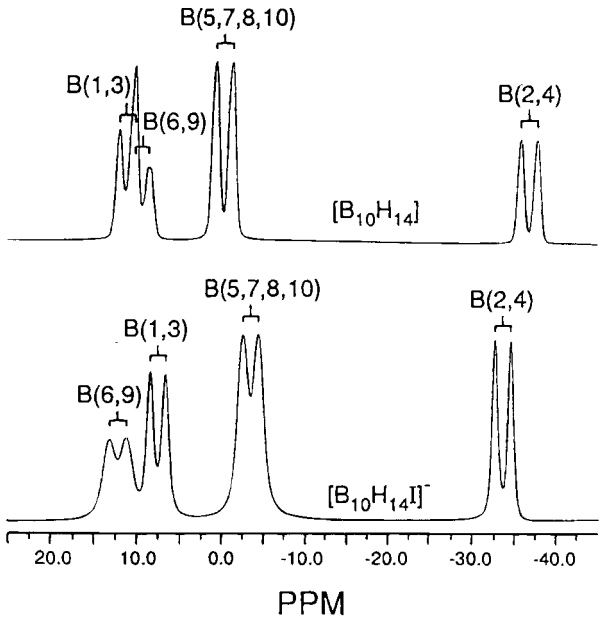

Figure 2. ^{11}B NMR spectra of $B_{10}H_{14}$ and $[B_{10}H_{14}I]^-$.

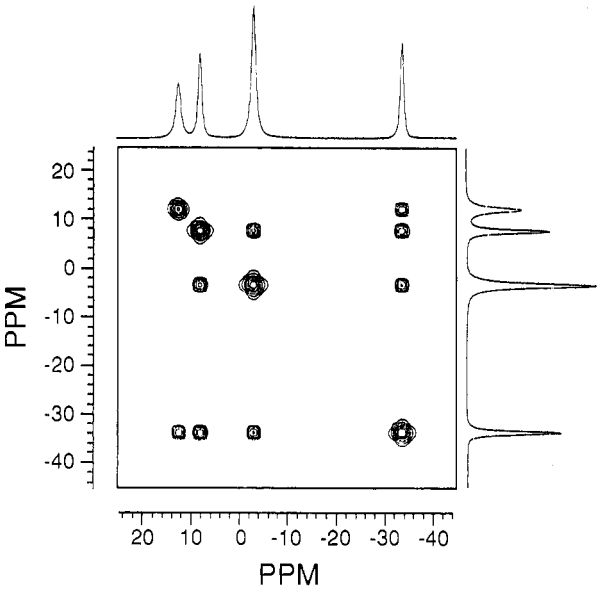

Figure 3. $^{11}B-^{11}B$ COSY spectrum for $[B_{10}H_{14}I]^-$.

boron spin-decoupling experiments, also shows perturbations with respect to the ^1H NMR spectrum of $B_{10}H_{14}$ in CD_2Cl_2: H(1,3) and H(5,7,8,10) are shifted upfield by 0.52 and 0.35 ppm, respectively, and H(6,9) and μ-H are each shifted downfield by 0.21 and 0.79 ppm, respectively. ^1H NMR spectra were obtained down to −90 °C with no significant change in the spectra.

The B−H stretching regions of the Raman spectra of solid $B_{10}H_{14}$ and solid $[(C_6H_5)_3P)_2N][B_{10}H_{14}I]$ show few differences in the values for the terminal B−H stretches (2400−2700 cm^{-1}). However, the bridging B−H−B stretches are shifted to lower energies in the spectrum of $[(C_6H_5)_3PMe][B_{10}H_{14}I]$ (ν_{B-H-B} = 1885, 1850 cm^{-1}) compared to that of $B_{10}H_{14}$ (ν_{B-H-B} = 1942, 1988 cm^{-1}). Solution Raman spectra in CH_2Cl_2 show the same shifts. Similar results are observed in the Raman spectra of $[(n\text{-}C_4H_9)_4N][B_{10}H_{14}I]$ and $[(C_6H_5)_3P)_2N][B_{10}H_{14}I]$.

The IR spectrum of $[(C_6H_5)_3PMe][B_{10}H_{14}I]$ shows a strong B−H stretching band at 2568 cm^{-1}, while the comparable band produced by $B_{10}H_{14}$ occurs at 2586 cm^{-1}.[5] Several weak absorptions are observed at 1883, 1840, 1816, and 1780 cm^{-1} for B−H−B stretching modes, while the comparable bands for $B_{10}H_{14}$ occur at 1939, 1896 cm^{-1}.[5]

$[2,4\text{-}I_2B_{10}H_{12}I]^-$. Formation of Complex Ions. X-ray studies of single crystals of $[P(C_6H_5)_3CH_3]^+$ and $[(C_6H_5)_3P)_2N]^+$ salts of the $[B_{10}H_{14}I]^-$ anion showed the B_{10} basket to be disordered. Therefore, to minimize the possibility for disorder in further X-ray investigations, the substituted decaborane 2,4-$I_2B_{10}H_{12}$ was employed. While no evidence for complex formation was obtained from mixing 2,4-$I_2B_{10}H_{12}$ with iodide salts in the absence of a solvent, the complex ion $[2,4\text{-}I_2B_{10}H_{12}I]^-$ was formed when 2,4-$I_2B_{10}H_{12}$ was stirred with an iodide salt in an appropriate solvent, according to eq 9.

$$MI + 2,4\text{-}I_2B_{10}H_{12} \rightarrow M[2,4\text{-}I_2B_{10}H_{12}I] \qquad (9)$$

$M = [N(n\text{-}C_4H_9)_4]^+$, $[P(C_6H_5)_3CH_3]^+$, $[(C_6H_5)_3P)_2N]^+$ in CH_2Cl_2

M = Na in THF

While 2,4-$I_2B_{10}H_{12}$ has limited solubility in CH_2Cl_2, addition of any of the iodide salts cited above causes the formation of a soluble product which is a deep orange complex compared to the light yellow color of 2,4-$I_2B_{10}H_{12}$. Solid salts of $[2,4\text{-}I_2B_{10}H_{12}I]^-$ show no sign of decomposition in air, but are unstable in solutions that are exposed to air.

X-ray Structure Determination. The structure of $[P(C_6H_5)_3CH_3][2,4\text{-}I_2B_{10}H_{12}I]$ was determined from a single crystal X-ray analysis. Figure 4 depicts the structure of the $[2,4\text{-}I_2B_{10}H_{12}I]^-$ anion. Bond distances and angles for $[2,4\text{-}I_2B_{10}H_{12}I]^-$ are collected in Tables 3 and 4, respectively. The unique iodine is situated at the open end of the B_{10} basket, effectively resting on the four bridging hydrogens. Structural parameters of the B_{10} framework are comparable to those of $B_{10}H_{13}I$[7] and $B_{10}H_{14}$[8] and the B−I distances B(2)−I(2) and B(4)−I(4) = 2.196(8)Å are comparable to those in $B_{10}H_{13}I$[7] and B_5H_8I.[9]

Spectra. ^{11}B NMR chemical shifts of $[2,4\text{-}I_2B_{10}H_{12}I]^-$ are summarized in Table 2. The assignments are based upon the trends observed in the spectra of $[B_{10}H_{14}I]^-$ ion. The B(6,9) and B(1,3) resonances partially overlap and the downfield peak assigned to B(6,9) is broader which may be due to coupling with the bridging hydrogens. The 2D ^{11}B-^{11}B COSY spectrum of $[(C_6H_5)_3P)_2N][2,4\text{-}I_2B_{10}H_{14}I]$ in CH_2Cl_2 is fully consistent with the assignments (Figure 5). As observed for $[B_{10}H_{14}I]^-$ the signals due to individual boron atoms in the ^{11}B NMR spectrum of $[PPN][2,4\text{-}I_2B_{10}H_{12}I]$ in CD_2Cl_2 also appear at frequencies shifted from those found for 2,4-$I_2B_{10}H_{12}$. These perturbations are as follows: B(1,3), 5.0 ppm downfield; B(5,7,8,10), 4.4 ppm upfield; B(2,4), 3.9 ppm downfield; B(6,9), 0.3 ppm downfield.

The ^1H NMR spectrum of $[(C_6H_5)_3P)_2N][2,4\text{-}I_2B_{10}H_{12}I]$ in CD_2Cl_2 (Table 2) was assigned on the basis of selective heteronuclear boron spin-decoupling, and it is also perturbed compared to the ^1H spectrum of 2,4-$I_2B_{10}H_{12}$: H(6,9) and H(5,7,8,10) resonances shift upfield by 0.99 and 0.45 ppm, respectively, and those due to H(1,3) and μ-H are shifted

(5) Adams, R. M., *Boron, Metallo-Boron Compounds and Boranes*; Interscience Publishers: New York, 1964; p 532.
(6) Schaeffer, R. *J. Am. Chem. Soc.* **1957**, *79*, 2726.
(7) Sequeira, A.; Hamilton, W. C. *Inorg. Chem.* **1967**, *6*, 1281.
(8) (a) Kasper, J. S.; Lucht, C. M.; Harker, D. *Acta Crystallogr.* **1950**, *3*, 436. (b) Moore, E. B.; Dickerson, R. E.; Lipscomb, W. N. *J. Chem. Phys.* **1957**, *27*, 209.
(9) Hall, L. H.; Block, S.; Perloff, A. *Acta Crystallogr.* **1965**, *19*, 658.

Table 2. Summary of NMR Data

boron-11 NMR	B(5,7,8,10)	B(6,9)	B(1,3)	B(2,4)
$B_{10}H_{14}$[a]	0.7 (156)[e]	10.6 (171)[e]	12.2 (149)[e]	35.7 (149)[e]
[PPN][$B_{10}H_{14}I$][a]	−3.1 (148)	12.3 (157)	7.8 (143)	−33.5 (151)
[PPN][$B_{10}H_{14}I$][b]	−2.4	14.0	8.6	−31.4
[$P(C_6H_5)_3CH_3$][$B_{10}H_{14}I$][c]	−3.0	12.2	8.1	−33.7
Na[$B_{10}H_{14}I$][b]	−2.7	12.9	8.5	−32.8
2,4-$I_2B_{10}H_{12}$[a]	1.1 (154)	9.6 (151)	15.3	5.6 (s)
[PPN][2,4-$I_2B_{10}H_{12}I$][a]	−3.3 (144)	9.9[d]	10[d]	−41.7 (s)
[Ph_3PMe][2,4-$I_2B_{10}H_{12}I$][a]	−3.2	10.0[d]	10.1[d]	−41.9 (s)
Na[2,4-$I_2B_{10}H_{12}I$][b]	−4.8 (138)	10[d]	8[d]	−42.2 (s)

proton NMR	H(5,7,8,10)	H(6,9)	H(1,3)	H(2,4)	μ-H
$B_{10}H_{14}$	3.11	3.86	3.64	0.62	−2.08
[PPN][$B_{10}H_{14}I$]	2.76	4.07	3.12	0.65	−1.29
2,4-$I_2B_{10}H_{12}$	3.66	4.72	4.51		−1.06
[PPN][2,4-$I_2B_{10}H_{12}I$]	3.21	3.73	4.93		−0.13

[a] CD_2Cl_2. [b] THF. [c] CH_2Cl_2. [d] Not well resolved. [e] Chemical shift and coupling constant: ppm(Hz).

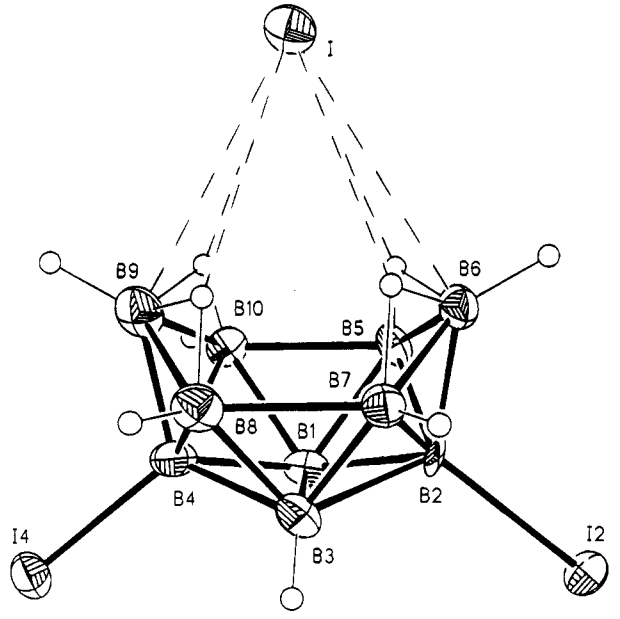

Figure 4. ORTEP plot of [2, 4-$I_2B_{10}H_{12}I$]$^-$.

Table 3. Selected Bond Distances (Å) and Esd's for the [2,4-$I_2B_{10}H_{12}I$]$^-$ Anion

B(1)−B(2)	1.781(11)	B(1)−B(3)	1.793(11)
B(1)−B(4)	1.719(12)	B(1)−B(5)	1.783(11)
B(1)−B(10)	1.733(11)	B(2)−B(3)	1.789(11)
B(2)−B(5)	1.753(11)	B(2)−B(6)	1.744(11)
B(2)−B(7)	1.821(11)	B(3)−B(4)	1.768(11)
B(3)−B(7)	1.746(11)	B(3)−B(8)	1.752(12)
B(4)−B(8)	1.795(12)	B(4)−B(9)	1.741(11)
B(4)−B(10)	1.781(11)	B(5)−B(6)	1.780(11)
B(5)−B(10)	1.975(11)	B(6)−B(7)	1.794(11)
B(7)−B(8)	1.949(12)	B(8)−B(9)	1.801(13)
B(9)−B(10)	1.775(12)		
I(2)−B(2)	2.181(7)	I(4)−B(4)	2.196(8)
B(1)−H(1)	0.98(6)	B(3)−H(3)	0.94(7)
B(5)−H(5)	1.13(7)	B(5)−H(11)	1.13(7)
B(6)−H(6)	1.13(7)	B(6)−H(11)	1.24(6)
B(6)−H(12)	1.33(7)	B(7)−H(7)	0.98(8)
B(7)−H(12)	1.28(7)	B(8)−H(8)	1.15(7)
B(8)−H(13)	1.17(7)	B(9)−H(9)	1.13(8)
B(9)−H(13)	1.39(7)	B(9)−H(14)	1.19(10)
B(10)−H(10)	1.11(6)	B(10)−H(14)	1.18(10)

downfield by 0.42 and 0.93 ppm, respectively. This spectrum is consistent with retention of the aparent C_{2v} symmetry of the 2,4-$I_2B_{10}H_{12}$ basket. Because of decomposition in the laser beam, the Raman spectrum of [2,4−$I_2B_{10}H_{12}I$]$^-$ could not be obtained. The IR spectrum shows one absorption at 2584 cm^{-1} and several bands at 1851, 1818, and 1778 cm^{-1} for B−H and B−H−B stretchings, respectively. The absorption for B−H stretching occurs at a frequency comparable with that for $B_{10}H_{14}$ (2586 cm^{-1})[5] and bands for B−H−B stretchings are lower in frequencies than the corresponding frequencies in $B_{10}H_{14}$ (1939, 1896 cm^{-1})[5]. The [2,4-$I_2B_{10}H_{12}I$]$^-$ ion absorbs in the visible region at 363 nm, while the starting material has an absorbance band at 329 nm.

Summary and Discussion

Decaborane(14) and the related molecule 2,4-$I_2B_{10}H_{12}$ react in 1:1 molar ratios with the iodide ion to form the ion-dipole charge transfer complexes [$B_{10}H_{14}I$]$^-$ and [2,4-I_2-$B_{10}H_{12}I$]$^-$. In the presence of large complex counterions [$B_{10}H_{14}I$]$^-$ and [2,4-I_2-$B_{10}H_{12}I$]$^-$ are remarkably thermally stable in the solid state. The boron hydrides cannot be sublimed from these solids up to decomposition temperatures (*ca.* 90 °C). In CH_2Cl_2 solutions evidence for interaction of the iodide ion with the $B_{10}H_{14}$ and 2,4-$I_2B_{10}H_{12}$ molecules is given by ^{11}B, ^{1}H, Raman, IR, and visible spectra. Job's continuous variations experiments demonstrate that [N(*n*-C_4H_9)$_4$]I and $B_{10}H_{14}$ react to form a stable complex in CH_2Cl_2 at room temperature that has a composition consistent with [N(*n*-C_4H_9)$_4$][$B_{10}H_{14}I$]. While the alkali metal iodides, NaI and KI, react with $B_{10}H_{14}$ in THF or EtOH solution to form [$B_{10}H_{14}I$]$^-$, removal of solvent results in dissociation into the alkali metal iodide and decaborane components. This dissociation is believed to reflect the expected relatively large lattice energies of the alkali metal iodides compared to those of the M[$B_{10}H_{14}I$] salts.

The molecular structure of the [2,4-$I_2B_{10}H_{12}$]$^-$ ion was determined as the [$P(C_6H_5)_3CH_3$]$^+$ salt. The iodide ion rests on the open face of the B_{10} basket. A space filling representation of this ion is given in Figure 6. Distances of the unique iodide atom to the bridge hydrogen atoms and the closest boron atoms B(6) and B(9) are given in Table 5. The average of the B(6)−I and B(9)−I distances, 3.528(8) Å , is significantly longer than the average of the B(4)−I(4) and B(2)−I(2) distances, 2.189(8) Å while the average of the unique iodide−bridging hydrogen distances, 3.06(7) Å, is longer than the sum of the H and I covalent radii, 1.70 Å.[21] However, these distances are consistent with van der Waals interactions. The sum of the H and I van der Waals radii falls within the range 3.2−3.6 Å.[10]

(10) (a) Bondi, A. *J. Phys. Chem.* **1964**, *68*, 441. (b) Cook. G. A. *Argon, Helium and the Rare Gases*; Wiley (Interscience): New York, 1961; Vol. I, p. 13. (c) Huheey, J. E.; Keiter, E. A.; Keiter, R. L. *Inorganic Chemistry* 4th ed.; Harper Collins College Publishers: New York, 1993; Table 8.1, p 292, footnote c.

Table 4. Selected Bond Angles (deg) and Esd's for the $[2,4\text{-}I_2B_{10}H_{12}I]^-$ Anion

B(2)−B(1)−B(3)	60.1(4)	B(2)−B(1)−B(4)	114.2(6)
B(2)−B(1)−B(5)	58.9(4)	B(2)−B(1)−B(10)	115.9(6)
B(3)−B(1)−B(4)	60.4(5)	B(3)−B(1)−B(5)	106.5(6)
B(3)−B(1)−B(10)	108.6(6)	B(4)−B(1)−B(5)	117.6(6)
B(4)−B(1)−B(10)	62.1(5)	B(5)−B(1)−B(10)	68.3(5)
I(2)−B(2)−B(1)	121.0(5)	I(2)−B(2)−B(3)	119.7(5)
I(2)−B(2)−B(5)	124.0(5)	I(2)−B(2)−B(6)	120.1(4)
I(2)−B(2)−B(7)	123.6(5)	B(1)−B(2)−B(3)	60.3(4)
B(1)−B(2)−B(5)	60.6(4)	B(1)−B(2)−B(6)	111.4(5)
B(1)−B(2)−B(7)	105.4(5)	B(3)−B(2)−B(5)	108.0(5)
B(1)−B(3)−B(2)	59.6(4)	B(1)−B(3)−B(4)	57.5(4)
B(2)−B(3)−B(4)	111.4(5)	B(1)−B(3)−B(7)	107.9(5)
B(2)−B(3)−B(7)	61.9(5)	B(4)−B(3)−B(7)	116.3(5)
B(1)−B(3)−B(8)	106.3(4)	B(2)−B(3)−B(8)	116.6(6)
B(4)−B(3)−B(8)	61.2(5)	B(7)−B(3)−B(8)	67.8(5)
B(1)−B(4)−B(3)	61.8(5)	B(1)−B(4)−B(8)	107.7(5)
B(3)−B(4)−B(8)	59.0(4)	B(1)−B(4)−B(9)	111.4(5)
B(3)−B(4)−B(9)	111.4(6)	B(8)−B(4)−B(9)	61.2(4)
B(1)−B(4)−B(10)	59.4(4)	B(3)−B(4)−B(10)	107.6(5)
B(8)−B(4)−B(10)	105.2(5)	B(9)−B(4)−B(10)	60.5(6)
I(4)−B(4)−B(1)	119.6(6)	I(4)−B(4)−B(3)	121.1(5)
I(4)−B(4)−B(8)	124.5(4)	I(4)−B(4)−B(9)	118.8(5)
I(4)−B(4)−B(10)	122.5(5)	B(1)−B(5)−B(2)	60.5(6)
B(1)−B(5)−B(6)	109.6(5)	B(2)−B(5)−B(6)	59.1(5)
B(1)−B(5)−B(10)	54.7(4)	B(2)−B(5)−B(10)	106.0(6)
B(6)−B(5)−B(10)	115.6(4)	B(2)−B(6)−B(5)	59.7(5)
B(2)−B(6)−B(7)	61.9(4)	B(5)−B(6)−B(7)	105.3(5)
B(2)−B(7)−B(3)	60.2(5)	B(2)−B(7)−B(6)	57.7(5)
B(3)−B(7)−B(6)	109.6(5)	B(2)−B(7)−B(8)	106.1(6)
B(3)−B(7)−B(8)	56.3(4)	B(6)−B(7)−B(8)	116.2(6)
B(3)−B(8)−B(4)	59.8(4)	B(3)−B(8)−B(7)	55.9(6)
B(4)−B(8)−B(7)	105.6(5)	B(3)−B(8)−B(9)	109.3(5)
B(4)−B(8)−B(9)	57.9(6)	B(7)−B(8)−B(9)	116.0(6)
B(4)−B(9)−B(8)	60.9(5)	B(4)−B(9)−B(10)	60.9(5)
B(8)−B(9)−B(10)	105.3(6)	B(1)−B(10)−B(4)	58.5(5)
B(1)−B(10)−B(5)	57.0(4)	B(1)−B(10)−B(9)	109.1(6)
B(4)−B(10)−B(5)	105.7(5)	B(4)−B(10)−B(9)	58.6(5)
B(5)−B(10)−B(9)	116.5(6)		
B(2)−B(1)−H(1)	117.(3)	B(3)−B(1)−H(1)	131.(3)
B(4)−B(1)−H(1)	122.(3)	B(5)−B(1)−H(1)	111.(3)
B(10)−B(1)−H(1)	114.(3)	B(1)−B(3)−H(3)	132.(5)
B(2)−B(3)−H(3)	123.(4)	B(4)−B(3)−H(3)	118.(4)
B(7)−B(3)−H(3)	114.(4)	B(8)−B(3)−H(3)	111.(4)
B(1)−B(5)−H(5)	122.(3)	B(1)−B(5)−H(11)	127.(3)
B(2)−B(5)−H(5)	125.(3)	B(2)−B(5)−H(11)	100.(3)
B(6)−B(5)−H(5)	121.(3)	B(6)−B(5)−H(11)	43.(3)
B(10)−B(5)−H(5)	117.(3)	B(10)−B(5)−H(11)	93.(3)
B(2)−B(6)−H(6)	128.(4)	B(2)−B(6)−H(11)	96.(3)
B(2)−B(6)−H(12)	106.(3)	B(5)−B(6)−H(6)	122.(4)
B(5)−B(6)−H(11)	39.(3)	B(5)−B(5)−H(12)	123.(3)
B(7)−B(6)−H(6)	129.(4)	B(7)−B(6)−H(11)	117.(3)
B(7)−B(6)−H(12)	46.(3)	B(2)−B(7)−H(7)	119.(4)
B(2)−B(7)−H(12)	104.(3)	B(3)−B(7)−H(7)	125.(4)
B(3)−B(7)−H(12)	133.(3)	B(6)−B(7)−H(7)	112.(4)
B(6)−B(7)−H(12)	48.(3)	B(8)−B(7)−H(12)	94.(3)
B(3)−B(8)−H(8)	127.(4)	B(3)−B(8)−H(13)	128.(3)
B(4)−B(8)−H(8)	105.(4)	B(7)−B(8)−H(8)	118.(4)
B(7)−B(8)−H(13)	88.(3)	B(9)−B(8)−H(8)	117.(4)
B(9)−B(8)−H(13)	51.(3)	B(4)−B(9)−H(9)	132.(4)
B(4)−B(9)−H(13)	99.(3)	B(4)−B(9)−H(14)	101.(5)
B(8)−B(9)−H(9)	124.(4)	B(8)−B(9)−H(13)	41.(3)
B(10)−B(9)−H(9)	123.(5)	B(10)−B(9)−H(13)	116.(3)
B(10)−B(9)−H(14)	41.(5)	B(1)−B(10)−H(10)	118.(3)
B(1)−B(10)−H(14)	133.(5)	B(4)−B(10)−H(10)	120.(3)
B(4)−B(10)−H(14)	99.(5)	B(5)−B(10)−H(10)	120.(3)
B(9)−B(10)−H(14)	99.(5)	B(9)−B(10)−H(14)	120.(3)
B(9)−B(10)−H(14)	42.(5)	B(5)−H(11)−B(6)	98.(5)
B(6)−H(12)−B(7)	87.(4)	B(8)−H(13)−B(9)	89.(5)
B(9)−H(14)−B(10)	97.(7)		

Decaborane is a polar molecule(3.17−3.62 D[11]). That the iodide ion rests upon the open face of the B_{10} basket is a reflection of the postive polar character of that end of the $B_{10}H_{14}$ molecule and its chemistry. The bridging hydrogens are

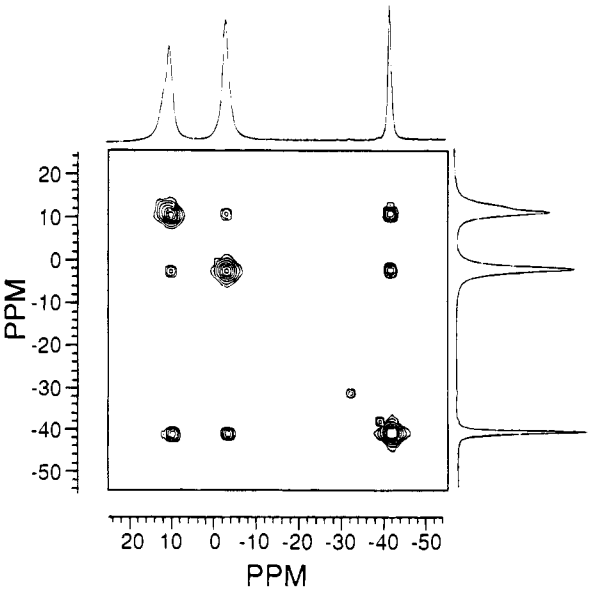

Figure 5. $^{11}B-^{11}B$ COSY spectrum for $[2,4\text{-}I_2B_{10}H_{12}I]^-$.

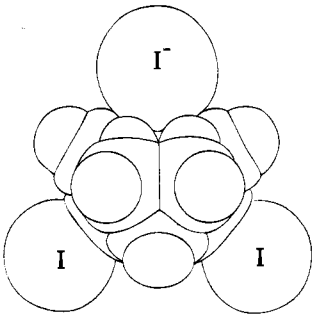

Figure 6. Space filling representation of $[2,4\text{-}I_2B_{10}H_{12}I]^-$.

Table 5. Distances (Å) to the Unique Iodide Atom

		Distances to $B_{10}H_{12}I_2$			
I−H(11)	3.11(7)	I−H(12)	2.99(7)	I−H(13)	3.05(8)
I−H(14)	3.10(7)	I−B(6)	3.526(8)	I−B(9)	3.530(7)
		Distances to Cation			
I−H(20)	3.23(6)	I−H(21)	3.10(7)	I−H(45)	3.27(7)
I−H(52)	3.41(6)	I−H(53)	3.22(7)		

Brönsted acids[12] and so the B(6) and B(9) sites are susceptible to nucleophilic attack.[13]

Many charge transfer complexes of the iodide ion are known.[15] In the present case the iodide ion is considered to transfer electronic charge to the LUMO of the electron deficient $B_{10}H_{14}$ molecule, a molecule that readily accepts one and two electrons.[14]

(11) (a) Bottei, R. S.; Laubengayer, A. W. *J. Phys. Chem.* **1961**, *66*, 1449. (b) Laubengayer, A. W.; Bottei, R. S. *J. Am. Chem. Soc.* **1952**, *74*, 1618.

(12) (a) Hawthorne, M. F.; Miller, J. J. *J. Am. Chem. Soc.* **1958**, *80*, 754. (b) Miller, J. J.; Hawthorne, M. F. *J. Am. Chem. Soc.* **1959**, *81*, 4501. (c) Shapiro, I.; Lustig, M.; Williams, R. *J. Am. Chem. Soc.* **1959**, *81*, 838. (d) Guter, G. A.; Schaeffer G. W. *J. Am. Chem. Soc.* **1956**, 78, 3546.

(13) (a) Van der Maas Redy, J.; Lipscomb, W. N. *J. Am. Chem. Soc.* **1959**, *81*, 754. (b) Van der Maas Redy, J.; Lipscomb, W. N. *J. Phys. Chem.* **1959**, 610. (c) Sands, D.; Zalkin, A. *Acta Crystallogr.* **1962**, *15*, 410.

(14) (a) Toeniskoetter, R. H.; Schaeffer, G. W. U.S. Pat. 2,921,833 (Jan 19, 1960). (b) Toeniskoetter, R. H.; Schaeffer, G. W.; Evers, E. C.; Hughes, R. E.; Bagley, G. E. *Abstracts of Papers*, 134th National Meeting of the American Chemical Society Chicago, IL, Sept 1958, American Chemical Society: Washington, DC, 1958; p 23N. (c) Toeniskoetter, R. H. *Diss. Abstr.* **1959**, *20*, 879.

(15) Kosower, E. M. *Molecular Biochemistry*; McGraw Hill Book Co.: New York, 1962; Section 2.13C.

Table 6. Crystallographic Data Summary

chem formula	$C_{19}H_{30}B_{10}I_3P$	β, deg	99.40(2)
fw	778.23	V, Å^3	2950.7
cryst syst	monoclinic	Z	4
space group	$P2_1/c$	radiation (λ, Å)	Mo Kα (0.710 69)
temp, °C	−162	$d_{calcd.}$, g cm^{-3}	1.752
a, Å	12.868(4)	abs coeff (μ), cm^{-1}	32.067
b, Å	10.562(3)	R^a	0.034
c, Å	22.007(8)	$R_w{}^b$	0.036

^{a} $R = \Sigma(|F_o| - |F_c|)/\Sigma|F_o|$. ^{b} $Rw = [\Sigma w(|F_o| - |F_c|)^2/\Sigma w|F_o|^2]^{1/2}$.

Experimental Section

Apparatus. All manipulations were carried out on a standard glass high vacuum line or in a glovebox under an atmosphere of dry, oxygen-free nitrogen. Boron-11 NMR spectra were obtained using a Nicolet NIC-500 or a Bruker AM 250 spectrometer operating at 160.4 MHz or 80.2 MHz, respectively. ^{1}H NMR spectra were obtained using a Bruker WM-300 spectrometer operating at 300.1 MHz. All IR spectra were recorded with 2-cm^{-1} resolution using a Mattson-Polaris FT-IR spectrometer. Visible spectra were obtained using a coherent argon ion laser with an excitation wavelength of 514.5 nm. The scattering light was passed through a Spex 1403 monochromator to obtain the spectrum.

Materials. $B_{10}H_{14}$ was prepared from B_5H_9 using the method of Toft and Shore.[16] 2,4-$I_2B_{10}H_{12}$ was prepared by iodination of $B_{10}H_{14}$ as described in the literature.[17] $[(C_6H_5)_3P)_2N]$[I] was prepared by metathesis of the corresponding chloride salt with KI in water. The insoluble $[(C_6H_5)_3P)_2N]$I was filtered, recrystallized from CH_2Cl_2 and Et_2O, and dried by heating under vacuum. $[P(C_6H_5)_3CH_3]$I was prepared by the reaction of excess MeI with PPh_3 in Et_2O as previously described in the literature.[18] The salt was recrystallized from CH_2Cl_2 and Et_2O before use. $[(n\text{-}C_4H_9)_4N]$I and NaI were purchased from Matheson, Coleman and Bell. These salts were dried by heating under vacuum prior to use. CH_2Cl_2 was distilled from P_2O_5 and stored under vacuum prior to use. THF and Et_2O were distilled from Na−benzophenone prior to use and stored under vacuum. Pentane was distilled from CaH_2 and stored under vacuum. Elemental analyses were performed by Schwarzkopf Microanalytical Laboratories, Woodside, NY.

Job's Experiment. The formation of the $[(n\text{-}C_4H_9)_4N][B_{10}H_{14}I]$ complex in CH_2Cl_2 was followed using Job's continuous variations method[1] by monitoring the absorbance maximum of the complex (355 nm). Ten 0.002 M solutions of [TBA]I and $B_{10}H_{14}$ were prepared in the glovebox with molar ratios of $[TBA^+I^-]/\{[TBA^+I^-]+[B_{10}H_{14}]\}$ equal to 0.1, 0.2, 0.3, 0.4, 05, 0.6, 0.7, 0.8, 0.9, and 1.0. Three sets of spectra were obtained using a 1.0-cm quartz cell in a thermostated cell compartment under a blanket of N_2 gas on a Varian 2300 recording spectrometer at 281, 268, and 250 K respectively. Absorbance *vs* molar fraction of [TBA]I was plotted. Three curves at different temperatures show maxima at 0.5 indicating that a 1:1 complex is formed. These curves were subjected to nonlinear fitting where equilibrium contants were derived.

X-ray Determination of $[P(C_6H_5)_3CH_3][2,4\text{-}I_2B_{10}H_{12}I]$. Crystallographic data for $[P(C_6H_5)_3CH_3][2,4\text{-}I_2B_{10}H_{12}I]$ are summarized in Table 6. Atomic positional parameters for $[2,4\text{-}I_2B_{10}H_{12}I]^-$ are presented in Table 7. In a N_2-filled glovebag, a transparent yellow crystal was cleaved to form a nearly equidimensional cube of approximate dimensions 0.14 × 0.13 × 0.15 mm. The crystal was affixed to a glass fiber using silicone grease and transferred, under N_2, to a Picker four-circle goniostat[19] where it was cooled to −162 °C. A systematic search of a limited hemisphere of reciprocal space located a set of diffraction maxima of 2/*m* symmetry with systematic extinctions consistent with space group $P2_1/c$. Data were corrected for background, Lorentz, and polarization effects; no absorption correction was applied.

The three iodine atoms were located from a Patterson synthesis using an interactive search program,[20] and all remaining atoms were located in successive Fourier syntheses and refined using anisotropic displacement parameters. All hydrogen atoms were located and refined isotropically. Neutral scattering factors were utilized and real dispersion corrections were included. A final difference Fourier was featureless, the largest peak being 0.32 e Å^{-3}.

Table 7. Positional Parameters and Esd's for the $[2,4\text{-}I_2B_{10}H_{12}I]^-$ Anion

atom	x	y	z	B_{iso},^{a,b} Å^2
B(1)	0.7059(6)	−0.0266(8)	0.4611(4)	16
B(2)	0.6094(5)	−0.1201(8)	0.4141(3)	16
B(3)	0.6745(7)	−0.1815(8)	0.4861(4)	19
B(4)	0.8006(6)	−0.1131(8)	0.5075(4)	20
B(5)	0.7023(6)	−0.0363(8)	0.3799(4)	18
B(6)	0.6605(6)	−0.1902(8)	0.3536(4)	19
B(7)	0.6587(7)	−0.2817(8)	0.4221(4)	18
B(8)	0.7860(7)	−0.2757(8)	0.4838(4)	22
B(9)	0.8911(7)	−0.1777(9)	0.4654(4)	24
B(10)	0.8315(6)	−0.0301(8)	0.4422(4)	17
I(2)	0.44260(3)	−0.07131(5)	0.40288(2)	22
I(4)	0.85592(4)	−0.05047(5)	0.60241(2)	22
I	0.90191(4)	−0.29912(5)	0.31714(2)	22
H(1)	0.684(4)	0.058(5)	0.473(2)	0(11)
H(3)	0.638(5)	−0.209(7)	0.518(3)	25(16)
H(5)	0.685(5)	0.049(6)	0.349(3)	16(14)
H(6)	0.619(5)	−0.209(7)	0.305(3)	24(15)
H(7)	0.608(6)	−0.352(7)	0.415(3)	29(16)
H(8)	0.810(6)	−0.365(7)	0.512(3)	24(16)
H(9)	0.977(6)	−0.201(7)	0.479(3)	30(17)
H(10)	0.879(5)	0.058(6)	0.449(3)	12(13)
H(11)	0.734(5)	−0.115(6)	0.354(3)	14(13)
H(12)	0.709(6)	−0.295(7)	0.377(3)	28(16)
H(13)	0.835(5)	−0.286(7)	0.443(3)	25(16)
H(14)	0.881(7)	−0.109(9)	0.422(4)	55(23)

^{a} Isotropic values for those atoms refined anisotropically are calculated using the formula given by: Hamilton, W. C. *Acta. Crystallogr.* **1959**, *12*, 609. ^{b} B_{iso} values are × 10.

Preparation of $[P(C_6H_5)_3CH_3][B_{10}H_{14}I]$. In the glovebox, a 30 mL flask was charged with 104 mg of $[(C_6H_5)_3CH_3P]$I and 31.5 mg of $B_{10}H_{14}$ (0.258 mmol). The flask was attached to a vacuum filtration apparatus using Solv-seal joints. The vessel was evacuated on the vacuum line and 2 mL of CH_2Cl_2 was admitted by condensing it at −196 °C. Warming to room temperature and stirring produced a deep yellow solution. The vessel was then cooled to −78 °C. Et_2O (2 mL) and pentane (2 mL) were admitted. Stirring precipitated a deep yellow solid. The solid was filtered and dried, affording 118 mg of a fine yellow powder.

The solid state Raman spectrum in the B−H stretching region (*ca.* 1600−2800 cm^{-1}) shows bands at 1847 (w), 1868 (m, sh), 1882 (m), 2014 (w), 2113 (s), 2204 (s), 2237 (m), 2577 (s) and 2607 (s) cm^{-1}. The peaks at 2014, 2113, 2204, and 2237 cm^{-1} are attributed to the $[P(C_6H_5)_3CH_3]^+$ cation. IR (CH_2Cl_2): 2568 (vs), 1883 (w), 1840 (w), 1816(w), 1780 (w), 1588 (m), 1510(s), 1485 (m), 1439 (s), 1414 (m), 1396 (m), 1337 (m), 1316 (m), 1191 (w), 1165 (w), 1156 (vs), 1008 (m), 998 (m), 926 (m), 902 (s), 852 (m), 812 (m), 786 (m), 686 (s), 652 (m), 626 (m), 507 (s), 488 (s) cm^{-1}. Anal. Calcd: B, 20.42; C, 43.0; H, 6.79; I, 23.95; P, 5.84. Found: B, 20.64; C, 42.44; H, 5.91; I, 22.86; P, 5.85. A similar procedure is used to prepare the $[(n\text{-}C_4H_9)_4N]^+$ and $[PPN]^+$ analogues.

Stability Tests on $[(C_6H_5)_3P)_2N][B_{10}H_{14}I]$. In the glovebox, 37.9 mg of $B_{10}H_{14}$ (0.325 mmol) and 218 mg of $[(C_6H_5)_3P)_2N]$[I] (0.325 mmol) were weighed into a 125 mL bulb equipped with a Kontes stopcock adaptor. The vessel was evacuated and 5 mL of CH_2Cl_2 was

(16) (a) Leach, J. B.; Toft, M. A.; Himpsl, F. L.; Shore, S. G. *J. Am. Chem. Soc.* **1981**, *103*, 988. (b) Toft, M. A.; Leach, J. B.; Himpsl, F. L.; Shore, S. G. *Inorg. Chem.* **1982**, *21*, 1952.

(17) Hillman, M. *J. Am. Chem. Soc.* **1960**, *82*, 1097.

(18) (a) Hertz, R. K. Ph.D. Dissertation, The Ohio State University, 1976. (b) Ryschkewitsch, G. E.; Nainan, K. C. *Inorg. Synth.* **1974**, *15*, 113.

(19) Data were collected at the Molecular Structure Center, Indiana University, Department of Chemistry. The diffractometer utilized for data collection (Picker four-circle goniostat equipped with a Furans monochromator (HOG crystal) and Picker X-ray generator) was designed and constructed at Indiana University.

(20) The Patterson function was interpreted by using TRISH, an interactive Patterson interpreter written by T. Curtis, and M. Hafely, Indiana University 1982.

(21) Wells, A. F. *Inorganic Chemistry*, 5th ed.; Clarendon Press: Oxford, England, 1984; p 289.

admitted by condensing it at −196 °C. Warming the solution to −78 °C and stirring caused the formation of the desired complex. The solvent was then removed by pumping it away at −35 °C. When all the CH_2Cl_2 had been removed, a sublimation probe having a water-cooled cold finger was fitted to the reaction vessel. No $B_{10}H_{14}$ could be sublimed from the complex under high vacuum at 50 °C. Raising the temperature to 90−95 °C yielded only trace amounts of $B_{10}H_{14}$ on the cold finger after several hours.

Preparation of $Na[B_{10}H_{14}I]$. In the glovebox were weighed 70.0 mg of $B_{10}H_{14}$ (0.573 mmol) and 85 mg of NaI (0.567 mmol) and placed into a 20 mL vessel equipped with a 5 mm NMR side tube. The vessel was evacuated on the vacuum line and 1−1.5 mL THF was condensed into the flask at −196 °C. The reaction vessel was then warmed to room temperature and the contents were stirred. The resulting deep yellow solution was tipped into the NMR tube and sealed off with a torch. The ^{11}B NMR spectrum consists of a doublet of area 4 at −2.7 ppm (J = 149 Hz) and three doublets of are 2 at −32.8 (J = 152 Hz), 8.5 (J = 143 Hz), and 12.9 (J = 158 Hz) ppm.

Several unsuccessful attempts were made to isolate this compound as a solid. Removal of THF from solutions of $[B_{10}H_{14}I]^-$ caused the bright yellow color to disappear as the solvent was being removed. $B_{10}H_{14}$ could then be readily sublimed from the vessel by pumping at room temperature. It appears that $Na[B_{10}H_{14}I]$ reverts to its starting materials as solvent is removed.

Preparation of $[(C_6H_5)_3P)_2N][2,4\text{-}I_2B_{10}H_{12}I]$. In the glovebox, 88.7 mg of 2,4-$B_{10}H_{12}I_2$ (0.237 mmol) and 158 mg of $[(C_6H_5)_3P)_2N]I$ (0.237 mmol) were weighed into a 30 mL bulb. The bulb was attached to a vacuum filtration apparatus using 9 mm Solv-seal joints. On the vacuum line, the vessel was evacuated and 2 mL of CH_2Cl_2 was condensed in at −196 °C. Warming and stirring caused the immediate formation of an orange solution. After overnight stirring at ambient temperature, 4 mL of Et_2O was condensed into the vessel at −78 °C. The resulting solution remained clear, even after several hours at −78 °C. Pumping to remove the solvent at about −50 °C, however, precipitated the complex. The solid was filtered and dried, yielding 218 mg of a free-flowing orange powder.

A sample for Raman spectroscopy was prepared. Although the solid sample was air stable, it decomposed in the laser beam. Several attempts to obtain the spectrum were unsuccessful. IR (CH_2Cl_2): 2584 (s), 1851 (w), 1818 (w), 1778 (w), 1589 (w), 1500 (w), 1484 (m), 1439 (m), 1318 (vs), 1250 (s), 1186 (m), 1116 (s), 998 (m), 870 (m), 854 (s), 794 (w), 757 (m), 716 (m), 686 (m), 548 (s), 535 (s), 501 (s) cm^{-1}.

A sample (0.217 mmol) in CD_2Cl_2 was prepared for ^1H and ^{11}B NMR studies. The ^{11}B NMR spectrum showed a singlet of relative area 2 at −41.7 ppm, a doublet of area 4 at −3.3 ppm (J = 144 Hz), and two overlapping signals of area 4 at 10−12 ppm. Proton spin-decoupling allows resolution of these overlapping peaks into two peaks at 11.0 ppm (J = 145 Hz) and 12.2 ppm.

Preparation of $Na[2,4\text{-}I_2B_{10}H_{12}I]$. In the glovebox, 65 mg of 2,4-$B_{10}H_{12}I_2$ (0.173 mmol) and 26.0 mg of NaI (0.173 mmol) were weighed into a 7 mL vessel equipped with a 5 mm NMR side tube. The vessel was evacuated on the vacuum line and 1−1.5 mL of THF was admitted by condensing it into the flask at −196 °C. Warming the flask to room temperature and stirring the contents for 5 min produced an orange-red solution. The solution was tipped into the NMR tube and sealed off with a torch. The sample was stored at −78 °C. The ^{11}B NMR spectrum consisted of a singlet of area 2 at −42.2 ppm, a doublet of area 4 at −4.8 ppm (J = 138 Hz), and two overlapping peaks at 8 ppm and 10 ppm. Proton spin-decoupling did not resolve the two downfield peaks. Samples which were allowed to stand at room temperature for several days were found to decompose to species which could not be identified by ^{11}B NMR studies.

Attempts were made to isolate $Na[2,4\text{-}I_2B_{10}H_{12}I]$ as a solid compound. An orange solid could be precipitated by slowly distilling pentane at 78 °C into a reaction vessel containing a solution of $Na[2,4\text{-}I_2B_{10}H_{12}I]$ in THF. Using a vacuum filtration apparatus, the orange solid could be filtered. However, complete removal of the solvent caused the color of the compound to change from orange to off-white. Exposing the vessel to THF solvent vapors at 100 Torr caused the immediate restoration of the orange color. The complex reverted to the starting materials in the absence of solvent.

Acknowledgment. We thank the Army Research Office (Grant DAAL03-92-G-0199) for support. NMR spectra were obtained at The Ohio State University Campus Chemical Instrument Center (funded in part by NSF Grant 79-10019 and NIH Grant 1 S10 PRO14512801A).

Supplementary Material Available: Tables of atomic coordinates, bond distances and angles for the $[P(C_6H_5)_3CH_3]^+$ cation, and anisotropic displacement parameters for $[P(C_6H_5)_3CH_3][2,4\text{-}I_2B_{10}H_{12}I]$ and figures showing the packing of the molecule and the structure of the cation (10 pages). Ordering information is given on any current masthead page.

IC941331D